Longitudinal Nuclear Spin Relaxation of *Ortho*- and *Para*-Hydrogen Dissolved in Organic Solvents

Christie Aroulanda,[†] Larisa Starovoytova,[‡] and Daniel Canet*[,†]

Méthodologie RMN (UMR CNRS-UHP 7565), Nancy-Université, Faculté des Sciences, BP 239, 54506 Vandoeuvre-lès-Nancy Cedex, France, and Department of Structure Analysis, Institute of Molecular Chemistry AV CR, v.v.i., Heyrovskeho nam. 2, 162 06 Praha-6, Czech Republic

Received: April 24, 2007; In Final Form: August 3, 2007

The longitudinal relaxation time of *ortho*-hydrogen (the spin isomer directly observable by NMR) has been measured in various organic solvents as a function of temperature. Experimental data are perfectly interpreted by postulating two mechanisms, namely intramolecular dipolar interaction and spin−rotation, with activation energies specific to these two mechanisms and to the solvent in which hydrogen is dissolved. This permits a clear separation of the two contributions at any temperature. Contrary to the self-diffusion coefficients at a given temperature, the rotational correlation times extracted from the dipolar relaxation contribution do not exhibit any definite trend with respect to solvent viscosity. Likewise, the spin−rotation correlation time obeys Hubbard's relation only in the case of hydrogen dissolved in acetone-d_6, yielding in that case a spin−rotation constant in agreement with literature data. Concerning *para*-hydrogen, which is NMR-silent, the only feasible approach is to dissolve *para*-enriched hydrogen in these solvents and to follow the back-conversion of the *para*-isomer into the *ortho*-isomer. Experimentally, this conversion has been observed to be exponential, with a time constant assumed to be the relaxation time of the singlet state (the spin state of the *para*-isomer). A theory, based on intermolecular dipolar interactions, has been worked out for explaining the very large values of these relaxation times which appear to be solvent-dependent.

Introduction

Until now, a very limited number of publications has dealt with nuclear spin relaxation and dynamics of hydrogen dissolved in liquids[1−3] and, in particular, little attention was paid to the relaxation mechanisms. Very recently, interesting experimental results concerning normal hydrogen (*ortho*-hydrogen) in various solvents and as a function of temperature have been published.[3] These authors show unambiguously the presence of two relaxation mechanisms: the intramolecular dipolar interaction (between the two hydrogen atoms of the hydrogen molecule) and the so-called spin−rotation (which stems from the coupling between the nuclear spin momentum and the molecular angular momentum).[3,4−10] As these two mechanisms have opposite temperature dependencies, they can be clearly identified. In fact, ref 3 appeared when the present study was in progress.[11] Here, our purpose is to characterize the relaxation mechanisms operative for *ortho*-hydrogen, but also for *para*-hydrogen. This is motivated by recent publications making use of *para*-hydrogen with the aim to improve the sensitivity of NMR experiments[12−17] and even MRI experiments.[18−21] In these latter experiments, hydrogen enriched in its *para*-isomer is first used for hydrogenating a substrate in which the two protons become nonequivalent and thus capable of releasing hyperpolarization.[16] It is therefore interesting to have insights into spin relaxation of the two species involved in the hydrogenation process, namely the two spin isomers of molecular hydrogen.

In this paper we demonstrate that, although nuclear spins relax quite differently in *ortho*- and *para*-hydrogen, the solvent is of prime importance. In *ortho*-hydrogen, usual relaxation mechanisms (intramolecular dipolar and spin−rotation) are observed whereas subtle cross-correlation spectral densities are involved in the relaxation of the singlet state (*para*-hydrogen).[17,22−24] Indeed, we shall focus on the back-conversion of *para*-hydrogen to *ortho*-hydrogen and provide time constants which are believed to be the *para*-hydrogen relaxation times.

Experimental Section

All relaxation experiments have been performed with a homemade 200 MHz NMR spectrometer (easily available for long periods). For normal hydrogen dissolved in organic solvents, the temperature was varied in the range allowed by the solvent melting and boiling points. *Para*−*ortho* conversion experiments have been carried out at ambient temperature (ca. 20 °C) for all solvents. For some of them, additional measurements at higher temperatures showed the expected behavior.

Self-diffusion coefficients were measured according to the standard PGSTE sequence (Pulsed Gradient Field Stimulated Echo with bipolar gradients) at ambient temperature using a Bruker DRX-400 spectrometer equipped with a 5 mm TBIZ probe.

The solvents employed in this work are all of commercial provenance, used without any further purification and directly weighted into o.d. 5 mm NMR tubes fitted with J-Young valves. These solvents are carbon disulfide (apolar), acetone-d_6, acetonitrile-d_6, and bromoethane-d_5 (polar and aprotic), and methanol-d_4, ethanol-d_6, and isopropanol-d_8 (polar and protic). The low solubility of hydrogen in common organic solvents entails a weak proton NMR signal which could not be easily observed in the presence of solvents signals of usual amplitude. The use

* Corresponding author. E-mail: Daniel.Canet@rmn.uhp-nancy.fr. Phone number: +33 3 83 68 43 49. Fax: +33 3 83 68 43 47.
[†] Nancy-Université.
[‡] Institute of Molecular Chemistry.

10.1021/jp073162r CCC: $37.00
Published on Web 10/03/2007

of deuterated solvents is therefore almost mandatory, and their residual proton signal serves as chemical shift reference. In the case of hydrogen dissolved in carbon disulfide, a drop of tetramethylsilane, TMS, has been added to the solution for NMR internal referencing.

Before dissolving hydrogen, the NMR samples were carefully degassed by at least three 10 min freeze−pump−thaw cycles. Normal hydrogen was directly transferred through the vacuum/hydrogen line into the NMR samples at about 1.5 bar.

Para-enriched hydrogen was obtained by storing normal hydrogen at 77 K in the presence of activated charcoal for 2−3 h.[25−28] Experimental details have already been reported elsewhere (see, for instance, ref 16). For studying the *para*−*ortho* conversion, the gas was directly transferred through the vacuum/hydrogen line at 0.6−1 bar, depending on the enrichment ratio experimentally achieved and on the solvent used.

Self-diffusion coefficients were determined by fitting experimental decays involving at least ten values of q ($q = \gamma_H g\delta/2\pi$, where γ_H is the proton gyromagnetic ratio, g is the incremented gradient strength, and δ is the duration of the gradient pulse). Longitudinal relaxation times T_1 were deduced from inversion−recovery experiments in a somewhat unusual manner: (i) equilibrium magnetization was obtained with a conventional one-pulse sequence with a waiting time of the order of $5T_1$ to ensure complete return to equilibrium, and (ii) two inversion−recovery measurements $\pi - \tau_{i(i=1,2)} - \pi/2$ were performed with τ_1 very small (e.g., 1 ms) and τ_2 of the order of T_1. These two experiments involve a dummy scan and a sufficient waiting time to avoid spin−echo formation. It can be shown that this choice of the τ_2 value minimizes the errors on T_1 values, calculated from the following equation:

$$T_1 = \frac{\tau_2}{\ln\left(\frac{M_0 - M_1}{M_0 - M_2}\right)} \tag{1}$$

where M_0, M_1, and M_2 are respectively the NMR signals corresponding to equilibrium and the first (τ_1) and second (τ_2) inversion−recovery experiments. Owing to the type of measurements dealt with in this paper, i.e., the determination of T_1 as a function of temperature with small temperature increments, this procedure has been run for obtaining rapidly accurate T_1 values, thus avoiding any spurious effect due to a possible drift of the temperature regulation device. To assess the accuracy of these determinations, the experiments were systematically repeated, at least twice.

***Ortho*-Hydrogen.** The evolution of R_1, the inverse of spin−lattice relaxation time T_1, as a function of temperature for the *ortho*-hydrogen dissolved in the solvents previously mentioned is in qualitative agreement with the work of Sartori et al.[3] who, however, used others solvents. There is a competition between the two possible relaxation mechanisms: intramolecular dipolar interaction and spin−rotation. As indicated above, the former is known to be less operative as temperature increases whereas the latter presents an opposite behavior.[5−10] This results in tiny variations in the considered range, and this implies very accurate measurements. Typical experimental data are shown in Figure 1a. They exhibit a characteristic shape that can be separated in three regions: (I) a decrease of R_1 at low temperature attributed to the decrease of dipolar contribution when temperature increases, (II) then a plateau indicating that the variations of the dipolar and spin−rotation mechanisms compensate almost each other, (III) and finally, at high temperature, a predominance of spin−rotation with an increase of the R_1 values with temperature. Qualitatively this behavior prevails for all the samples studied here (see Figure 1b) but the relative width and the position of these regions strongly depend on the solvent, namely region I may in some instances be shortened or even disappear (see carbon disulfide data).

To get some insight in these phenomena, we tentatively interpreted the experimental data according to the following expression:

$$R_1(T) = R_1^{\text{dip.}}(T) + R_1^{\text{sr}}(T) = h_d \exp(\lambda_d/T) + h_{sr} \exp(-\lambda_{sr}/T) \tag{2}$$

According to this model, h_d and h_{sr} represent the strength of the dipolar and spin−rotation mechanisms, respectively. h_d is proportional to $(1/r_{H-H})^6$ (where r_{H-H} is the interatomic distance in the hydrogen molecule), and h_{sr} is proportional to the square of the so-called spin−rotation constant.[4−10,29−36] In eq 2, we assume that the relevant processes can be characterized by an activation energy, namely λ_d for the molecular reorientation, and λ_{sr} for the spin−rotation, both quantities being positive. This means also that the prefactor of the Arrhenius law pertaining to these two mechanisms, is inserted in the parameters h_d and h_{sr}, respectively. The two processes are assumed to be independent although they both originate from the overall rotation of the hydrogen molecule. Concerning the dipolar interaction, the correlation time τ_c^d (proportional to $\exp(\lambda_d/T)$) indicates the correlation of orientations that evidently decreases when temperature increases. In the case of the spin−rotation interaction, the correlation time τ_c^{sr} (proportional to $\exp(-\lambda_{sr}/T)$) indicates the correlation of angular velocities because the molecular angular momentum is actually involved in this mechanism. This correlation increases when rotational motions become faster, thus when temperature increases.

Data have been fitted in the following way: λ_d and λ_{sr} are first estimated, h_d and h_{sr} are then deduced from a *linear* treatment of eq 2. These values of h_d and h_{sr} allow us to obtain new estimates of λ_d and λ_{sr} by a *nonlinear* fit (the SIMPLEX algorithm is used) which in turn leads to new values for h_d and h_{sr}, and so on. The results so obtained are shown in Figure 1b. Deviation between experimental and recalculated data are thought to be quite acceptable owing to the small variations with temperature and to the accuracy of measured quantities (we estimated an error of ca. 2−3%). All the results are gathered in Table 1. Owing to the prefactor alluded to above and to the ignorance of factors governing the spin−rotation constants, it seems illusory to discuss h_d and h_{sr} values (they are given in Table 1 merely for the sake of completeness). On the other hand, if Hubbard's law applies λ_d and λ_{sr} should be equal. This is seen to be verified for hydrogen dissolved in acetone-d_6 (see below for more details). Anyway, these parameters allow us to calculate, at each temperature, the "theoretical" dipolar contribution $R_1^{\text{dip.}}$, and the "theoretical" spin−rotation contribution R_1^{sr} rather than using raw experimental data. This can be seen as a smoothing procedure, allowing us to separate the contribution of each mechanism, which cannot be done directly from experimental data. Because we have assumed extreme narrowing (and this is very likely), $R_1^{\text{dip.}}$ is proportional to τ_c^d, and R_1^{sr} to τ_c^{sr} as indicated below:

$$R_1^{\text{dip.}}(T) = K_d \tau_c^d(T) \tag{3a}$$

$$R_1^{sr}(T) = TK_{sr}\tau_c^{sr}(T) \tag{3b}$$

In these equations, $K_d = {}^3/_2(\mu_0/4\pi)^2(\hbar\gamma_H{}^2/r_{H-H}{}^3)^2$ (homonuclear and intramolecular dipole−dipole case[7]), and $K_{sr} = (4Ik_B)/$

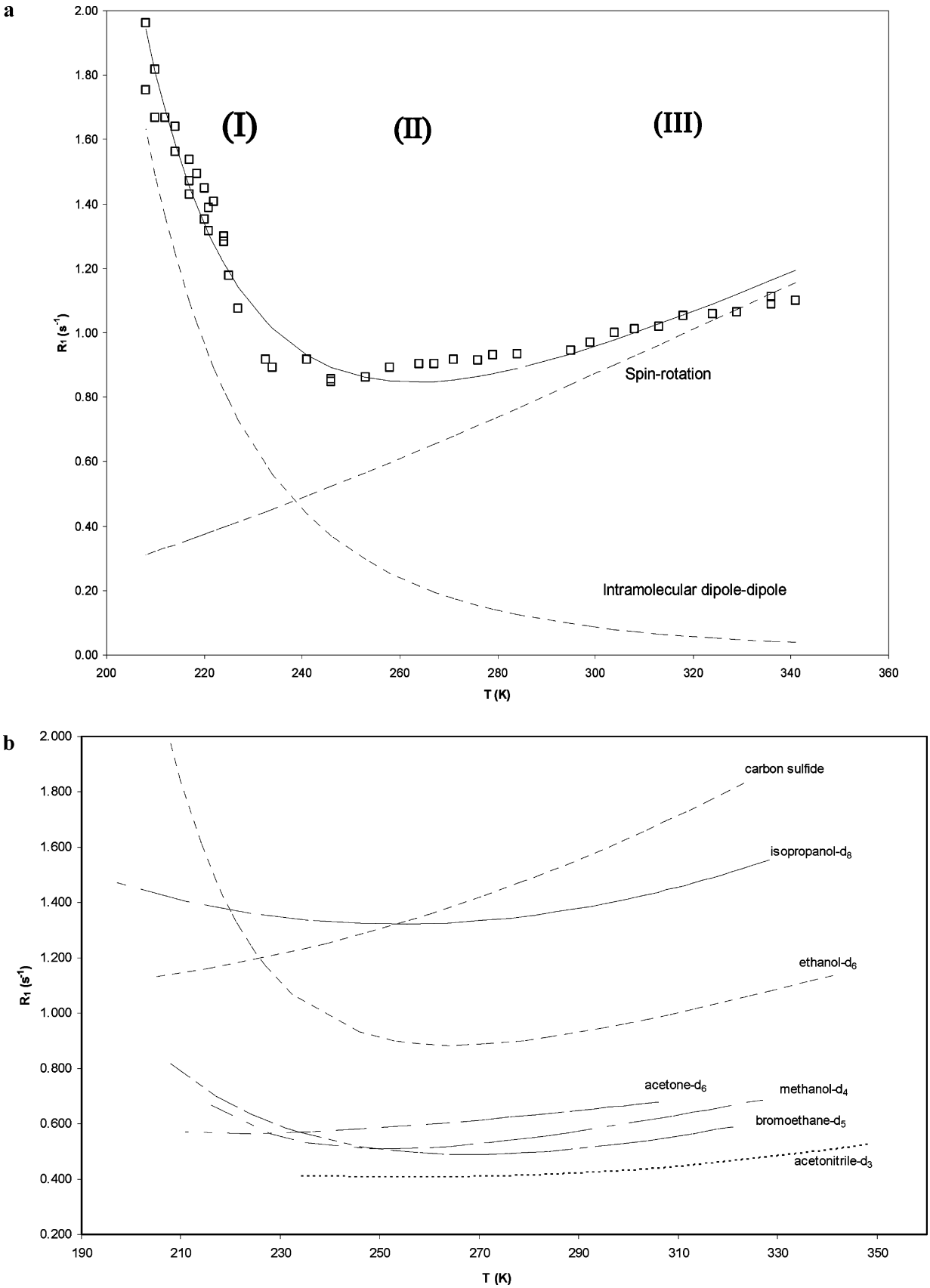

Figure 1. (a) Typical evolution, as a function of temperature, of the longitudinal relaxation rate R_1 of hydrogen dissolved in an organic solvent (here ethanol-d_6) with the three regions described in the text: (I) predominance of the intramolecular dipolar mechanism, (II) competition between dipolar and spin−rotation mechanisms, (III) predominance of the spin−rotation mechanism. Empty squares are the experimental data points. The dashed curves result from the fitting procedure described in the text (see eq 2). The solid line is the sum of the latter and represents the best fit to the experimental data. (b) Evolutions, as a function of temperature, of the longitudinal relaxation rate R_1 of hydrogen dissolved in the various organic solvents considered in this paper, represented here through recalculated curves as the one of Figure 1a.

TABLE 1: Intramolecular Dipole−Dipole and Spin−Rotation Relaxation Parameters

solvents	h_d (s^{-1})	λ_d (K)	h_{sr} (s^{-1})	λ_{sr} (K)	rms	λ_d/λ_{sr}
acetone-d_6[a]	5.29×10^{-3}	1026.87	10.96	1017.62	0.015	1.01
carbon disulfide[a,b]	n.a	n.a	2.7	134.7	0.003	n.a
acetonitrile-d_3[a]	6.68×10^{-3}	874.4	4.55	800.01	0.004	1.09
bromoethane-d_5[a]	1.69×10^{-2}	592.59	2.44	449.23	0.011	1.32
methanol-d_4[a]	1.03×10^{-4}	1788.86	4.08	594.94	0.024	3.01
ethanol-d_6[a]	5.19×10^{-5}	2144.56	5.10	521.08	0.051	4.12
isopropanol-d_8[a]	5.28×10^{-1}	179.26	54.10	1507.53	0.047	0.12

[a] Error estimated to ca. 2−3%. [b] In the case of carbon disulfide, available experimental data correspond only to zone III (spin−rotation predominance).

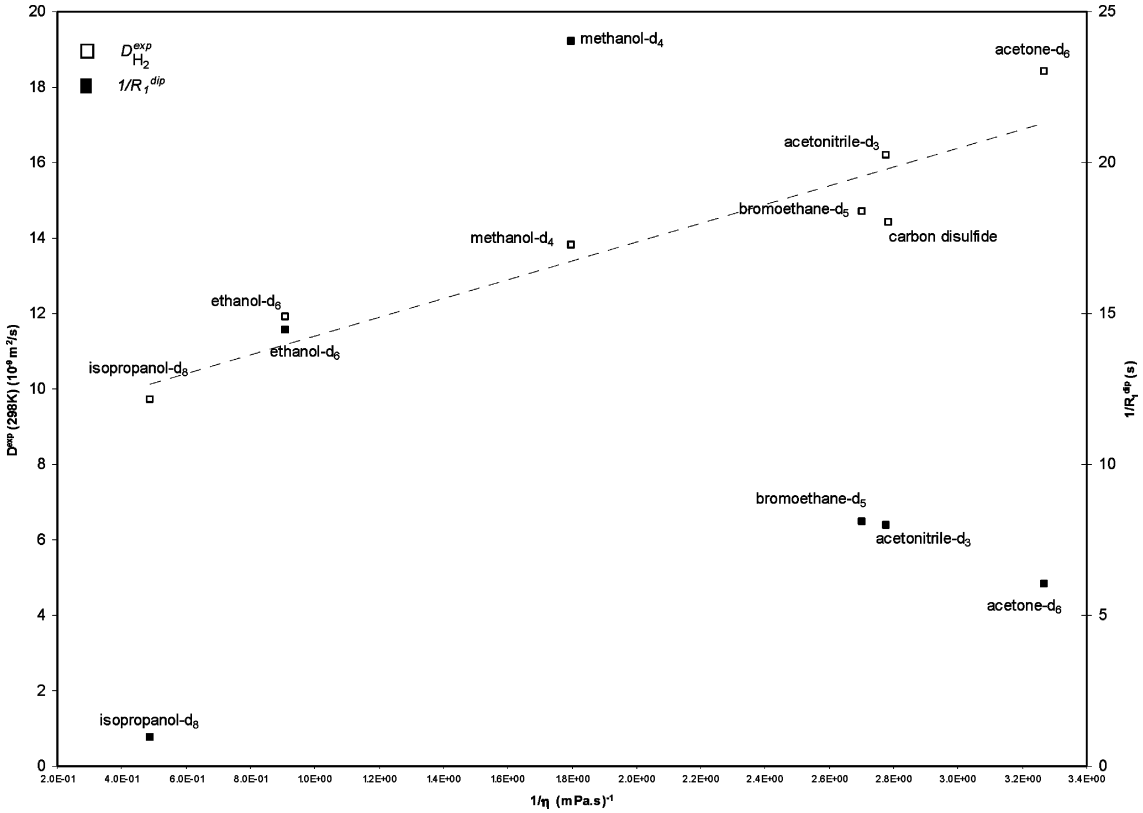

Figure 2. Evolution, as a function of the inverse of the viscosity, $1/\eta$, of $D^{exp}_{H_2}$ (self-diffusion coefficient, symbolized by empty squares) and of $1/R_1^{dip.}$ (intramolecular dipolar contribution to the longitudinal relaxation time, symbolized by full squares) for the hydrogen molecule dissolved in solvents of different viscosity at 298 K. As far as self-diffusion coefficients are concerned, the straight line has been obtained by linear regression.

$(3\hbar^2 C_{eff}^2)$, where I is the inertia moment of the hydrogen molecule (4.6×10^{-48} kg·m^2),[3,36] C_{eff} its effective spin−rotation constant.[8−10] The others symbols have their usual meanings.

We first discuss τ_c^d, which describes the tumbling of the hydrogen molecule in a given solvent. In Figure 2, $1/R_1^{dip.}$ at 298 K is shown as a function of the solvent viscosity and is compared to the self-diffusion coefficient, $D^{exp}_{H_2}$, of the hydrogen molecule in the same solvents. The experimental values obtained for $D^{exp}_{H_2}$(298K) in the various solvents studied here are reported in Table 2. $D^{exp}_{H_2}$ decreases when viscosity increases, indicating that the Stokes−Einstein (SE) law applies reasonably well in the case of *translational* motions according to the well-known relation given below:[10]

$$D^{exp}_{H_2}(T) = \frac{1}{6\pi}\frac{k_B T}{\eta r_{S,tr}} \qquad (4)$$

where η is the bulk viscosity of the solvent at the considered temperature, and $r_{S,tr}$ is the Stokes radius corresponding to the effective radius of the diffusing particle. From linear regression, we found $r_{S,tr} = 0.88$ Å. This value is consistent with the theoretically calculated bond length in the nonsolvated hydrogen molecule ($r_{H-H} = 0.74$ Å[36]) but smaller than its van der Waals radius (1.38 Å[3,40]). Remember that in principle, for the SE model, brownian spherical molecules of larger size than the solvent molecules are assumed, which is not really the case for the hydrogen molecule in the solvents considered here. Now, rotational motion can be probed by τ_c^d thus by $R_1^{dip.}$ (see eq 3a).

TABLE 2: *Ortho*-Hydrogen Self-Diffusion Coefficients Values Measured at 298 K in the Solvents Considered in This Work

solvent	$D^{exp}_{H_2}$(298K) (10^{-9} m^2 s^{-1})	η(298K)[a] (mPa s)
acetone-d_6	18.4	0.306
carbon disulfide	14.4	0.352
acetonitrile-d_3	16.2	0.369
bromoethane-d_5	14.7	0.374
methanol-d_4	13.8	0.544
ethanol-d_6	11.9	1.074
isopropanol-d_8	9.7	2.038

[a] Viscosity values have been obtained by modeling the experimental data available in ref 37 according to an Arrhenius type law (following ref 38). As usually done, the effect of isotopic labeling on the viscosity values has been neglected.[3]

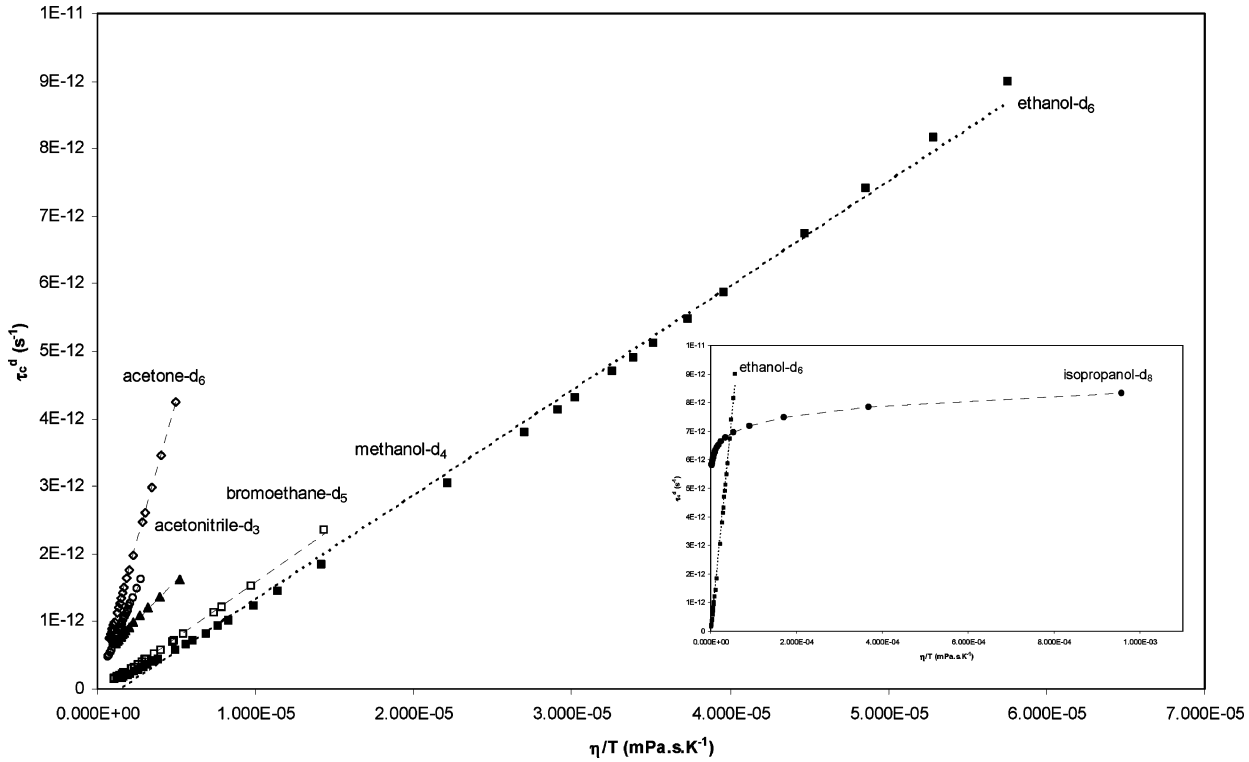

Figure 3. τ_c^dderived from the recalculated dipolar contribution (see eq 3a) as a function of η/T, for hydrogen dissolved in the solvents investigated in this work except carbon sulfide (no $R_1^{dip.}$ data available). Inset: data for isopropanol-d_8. The data set corresponding to hydrogen dissolved in ethanol-d_6 is shown for the sake of comparison. The straight lines have been obtained by linear regression.

We observe that, contrary to the self-diffusion coefficients, experimental data do not exhibit a linear behavior as a function of viscosity. The usual way of treating reorientational correlation times rests in the following equation:[10,41]

$$\tau_c^d = \tau_0 + \tau_{red.}\frac{\eta}{T} \quad (5)$$

The quantity $\tau_{red.}$ is usually denoted "reduced correlation time" whereas τ_0 corresponds to a possible inertial contribution. Plots of τ_c^d vs η/T, are shown in Figure 3. Reorientation of the hydrogen molecule in carbon disulfide is obviously not reported in this figure, just because the dipolar contribution in this solvent cannot be accurately determined. Otherwise, except in the case of isopropanol-d_8, plots are linear. This means that, (i) the model used is satisfactory (again except for hydrogen dissolved in isopropanol-d_8), (ii) the intercept, τ_0, is not significantly different from zero as expected.[41] Let us try to get some physical insights about the frictional coefficient $\tau_{red.}$. In the Stokes−Einstein−Debye (SED) model, the reorientational correlation time τ_c^d is proportional, in the stick boundary condition, to η/T as indicated below:[10,37−39]

$$\tau_c^d = \tau_{red.}\frac{\eta}{T} = \frac{V}{k_B}\frac{\eta}{T} \quad (6)$$

where V is the apparent molecular volume which could be taken as $(4\pi r_{S,tr}^3)/3$. According to this model, the slopes of the lines in Figure 3 should be identical. In fact, they are solvent dependent, which means that either the hydrodynamic radius that should be used for the rotational motion, $r_{S,rot.}$, is also solvent dependent or that we must introduce a microviscosity factor f such that η should be replaced by $f\eta$[10,41−43] (see below). Disregarding in a first approach the microviscosity concept, we can derive $r_{S,rot.}$ from the slopes of τ_c^d vs η/T (in the case of isopropanol-d_8, this quantity is calculated from τ_c^d at 298 K using eq 5). These apparent hydrodynamic radii are reported in Table 3 along with the rotational correlation times estimated from eq 3a. The values found are consistent with $r_{H-H} = 0.74$ Å[36] and with the van der Waals radius of the hydrogen molecule (1.38 Å[3,40]) but lie in a broad range. This probably means that the SED model is not completely adequate in describing the rotational motion of the system, especially for molecules submitted to long-range and/or specific solute−solvent interactions in addition to short-range interactions governed by the size of the molecules.[3] Another way to tackle the problem is to assume that the SED hydrodynamic radius, $r_{S,rot.}$ should be the same as the one determined by the self-diffusion coefficients through the SE-model (i.e., $r_{S,tr}$) and then to calculate the microviscosity coefficient f for each solvent. Three models have been proposed in the past for estimating the microviscosity factors.[41−44] Gierer and Wirtz assumed a spherical molecule,

TABLE 3: Rotational Correlation Times, Apparent Hydrodynamic Radii and Microviscosity Factors for the Hydrogen Molecule in the Solvents Considered Here

solvent	$\tau_c^{d,exp}$ (ps)[a]	$\tau_{red.}^{exp}$ (K mPa^{-1})[d]	$r_{S,rot.}$ (Å)[f]	f_{exp}[h]
acetone-d_6	0.96	8.39×10^{-7}	1.40	0.248
carbon sulfide[b]	n.a.	n.a.	n.a.	n.a.
acetonitrile-d_3	0.73	5.53×10^{-7}	1.22	0.375
bromoethane-d_5	0.71	2.34×10^{-7}	0.92	0.875
methanol-d_4	0.24	1.63×10^{-7}	0.81	1.282
ethanol-d_6	0.39	1.54×10^{-7}	0.80	1.331
isopropanol-d_8	6.12[c]	n.a.[e]	1.43[g]	0.233

[a] Calculated using eq 3a from the recalculated $R_1^{dip.}$ at 298 K. [b] No significant dipolar contribution available. [c] Calculated at 298 K using eq 3a. [d] Slopes of the plots τ_c^d vs η/T (see Figure 3). [e] τ_c^d vs η/T is not linear in the case of hydrogen dissolved in isopropanol-d_8. [f] Apparent hydrodynamic radius in the SED model, calculated from $\tau_{red.}^{exp} = (4\pi r_{S,rot.}^3)/(3k_B)$. [g] Calculated at 298 K from eqs 5 and 6. [h] $f_{exp} = \tau_c^{d,exp}/(V/k_B)$, where $V = 4\pi/3 r_{S,tr}^3$.

Hu and Zwanzig an axially symmetrical ellipsoid, and Youngren−Acrivos an ellipsoid without symmetry. As all these authors found microviscosity factors smaller than 1, it is obvious that such models cannot account for the rotational motion of hydrogen molecule in alcohols (the value corresponding to hydrogen in isopropanol-d_8 is deceptive because no linear behavior is observed in that case). As a matter of fact, Woessner[37] and others[38−39] explain that, in certain cases, viscosity has nothing to do with rotational correlation times. Concerning alcohols, one can of course invoke hydrogen bonds and a peculiar structure of the liquid state. For the others solvents, the apparent microviscosity factor should be discussed with regard to the Hu and Zwanzig model because the hydrogen molecule behaves very likely as a prolate ellipsoid. From theoretical values,[43] stick conditions would prevail with an eccentricity from 0.3 to 0.9 (which is probably not very meaningful). It can be mentioned that f values extracted from the Gierer and Wirtz model are an order of magnitude lower that the ones given in Table 3 and almost identical regardless of the solvent. This definitely precludes a spherical model for describing the hydrogen molecule as far as the rotational motion is concerned.

We turn now to the spin−rotation correlation time τ_c^{sr}, with regard to the rotational correlation time τ_c^{d}. Let us compare their evolution with temperature. As already mentioned, they evolve in opposite ways and Hubbard predicted that, for a given molecule assumed to be spherical and in the limit of small step diffusion, the product $\tau_c^{d}\tau_c^{sr}$ should be independent of solvent and proportional to the inverse of the absolute temperature.[4,6−10] According to eqs 3, these features can be checked by plotting $R_1^{dip}\cdot R_1^{sr}$ as a function of temperature (Figures 4). Indeed, owing to the Hubbard formula, $\tau_c^{d}\tau_c^{sr} = I/(6k_BT)$, we obtain the following relation:

$$R_1^{dip}\cdot R_1^{sr} = K_d K_{sr}\frac{I}{6k_B} = \left(K_d\frac{2I^2}{9\hbar^2}\right)C_{eff}^{\ 2} \qquad (7)$$

Moreover, from eq 2 it turns out that $R_1^{dip}\cdot R_1^{sr}$ is equal to $h_d h_{sr}\exp((\lambda_d - \lambda_{sr})/T)$. Henceforth, if Hubbard's predictions apply, we may have additional relationship between the various parameters, leading by identification with eq 6, to $\lambda_{sr} = \lambda_d$, and a constant value for the product $h_d h_{sr}$ if C_{eff} is constant. We first observe that $R_1^{dip}\cdot R_1^{sr}$ either is approximately constant for hydrogen dissolved in acetone-d_6 or varies linearly with temperature in acetonitrile-d_3 and bromoethane-d_5 over their whole temperature range (Figure 4a). However, the behavior is different when hydrogen is dissolved in alcohols (Figure 4b). Besides, if we consider the data in Table 1 for λ_d/λ_{sr}, we see that this ratio is not far from 1 for the nonalcoholic solvents but is erratic for the alcohols. Again, it seems that the spin dynamics of the hydrogen molecule dissolved in alcohols cannot be properly described by simple models. As already discussed, the exception of alcohols could be attributed to the existence of hydrogen bonds and would emphasize the dependence of spin−rotation constants upon the structure of the liquid state. Remember that, in Hubbard's model, the investigated solvent should not be too viscous, which is probably not the case for alcohols because of their ability to form an inter/intramolecular hydrogen bond network. Now, according to Hubbard's law, we should observe the same constant value whatever the (nonalcoholic) solvent used. The spin−rotation phenomenon is as usual described by a second-rank tensor, which can be experimentally determined by molecular beams, microwave spectroscopy experiments, or solid-state NMR experiments.[29−35,45] Due to the symmetry of the hydrogen molecule, this tensor reduces to a scalar denoted C_{eff}, that can be determined from experimental data by means of eq 7. Except for acetone-d_6, we can first notice that the product $R_1^{dip}\cdot R_1^{sr}$, thus C_{eff}, is temperature dependent. This indicates that Hubbard's mode is not valid here, because its conditions of application are not satisfied. This is not so surprising owing to its limited conditions of application. Others molecules for which rotational motion and spin−rotation are not linked through the Hubbard law, even in the diffusive regime, have been already mentioned.[41,47−49] Nevertheless, in the case of hydrogen dissolved in acetone-d_6, we can safely calculate C_{eff}; we obtain 132 kHz in satisfactory agreement with the literature value of 113.9 kHz.[31,32]

***Para*-Hydrogen.** Contrary to *ortho*-hydrogen, *para*-hydrogen is NMR silent because it corresponds to a singlet state (described by the wavefunction $1/\sqrt{2}(\alpha\beta - \beta\alpha)$, where α and β are the two proton nuclear spin functions) without any connection with the others spin states.[12,13] The equilibrium *para*−*ortho* hydrogen proportions are obviously temperature-dependent: the ratio between both isomers is theoretically 1:1 at 77 K whereas at ambient temperature it is 1:3 in favor of the *ortho*-isomer. Hence, if, after the *para*-enrichment of normal hydrogen performed at liquid nitrogen temperature (under atmospheric pressure), this *para*-enriched hydrogen is dissolved at ambient temperature in an organic solvent, we expect the return to equilibrium, i.e., a *para*−*ortho* proportion of 1:3, thus a back-conversion of the *para*-isomer toward the *ortho*-isomer. This conversion originates from relaxation phenomena and, more precisely, from relaxation mechanisms that act on the singlet state. This has been already studied[17,22−24] and will be further discussed below. For the moment, we shall consider experimental data that have been obtained by simply following the amplitude of the ^{1}H NMR peak of *ortho*-hydrogen as a function of time. In Figure 5a are reported some typical experimental curves featuring the *para*−*ortho* conversion. All the experimental data have been fitted according to the following exponential model:

$$S(t) = S_\infty\left[1 - \frac{k-1}{k}\exp\left(-\frac{t}{T_{p-o}}\right)\right] \qquad (8)$$

where $S(t)$ and S_∞ are respectively the *ortho*-hydrogen NMR signal recorded at time t after incorporation at ambient temperature of the *para*-enriched hydrogen into the considered solvent and at the end of the *para*−*ortho* conversion (i.e., at the thermodynamic equilibrium composition at ambient or higher temperature, see details for each sample in Table 4), k being the *para*-enrichment ratio experimentally achieved. Regarding the *para*−*ortho* equilibrium proportions at 77 K and at ambient temperature, the value of k is expected to lie in the range $0 < k \leq 3/2$. In this model, T_{p-o} denotes the time constant of the *para*−*ortho* conversion, which is nothing else than the hydrogen singlet-state relaxation time, because when a molecule ceases to be in the *para* state, it is necessary in the *ortho* state.

To gain more insight into the factors governing this relaxation phenomenon, we studied the *para*−*ortho* conversion of *para*-enriched hydrogen dissolved in the same organic solvents as in the previous section. Measurements were performed at ambient temperature (and sometimes at higher temperature), and also in the presence of paramagnetic ions. For a better legibility, experimental results are shown in Figure 5b in the form of "theoretical" curves deduced from experimental data points and

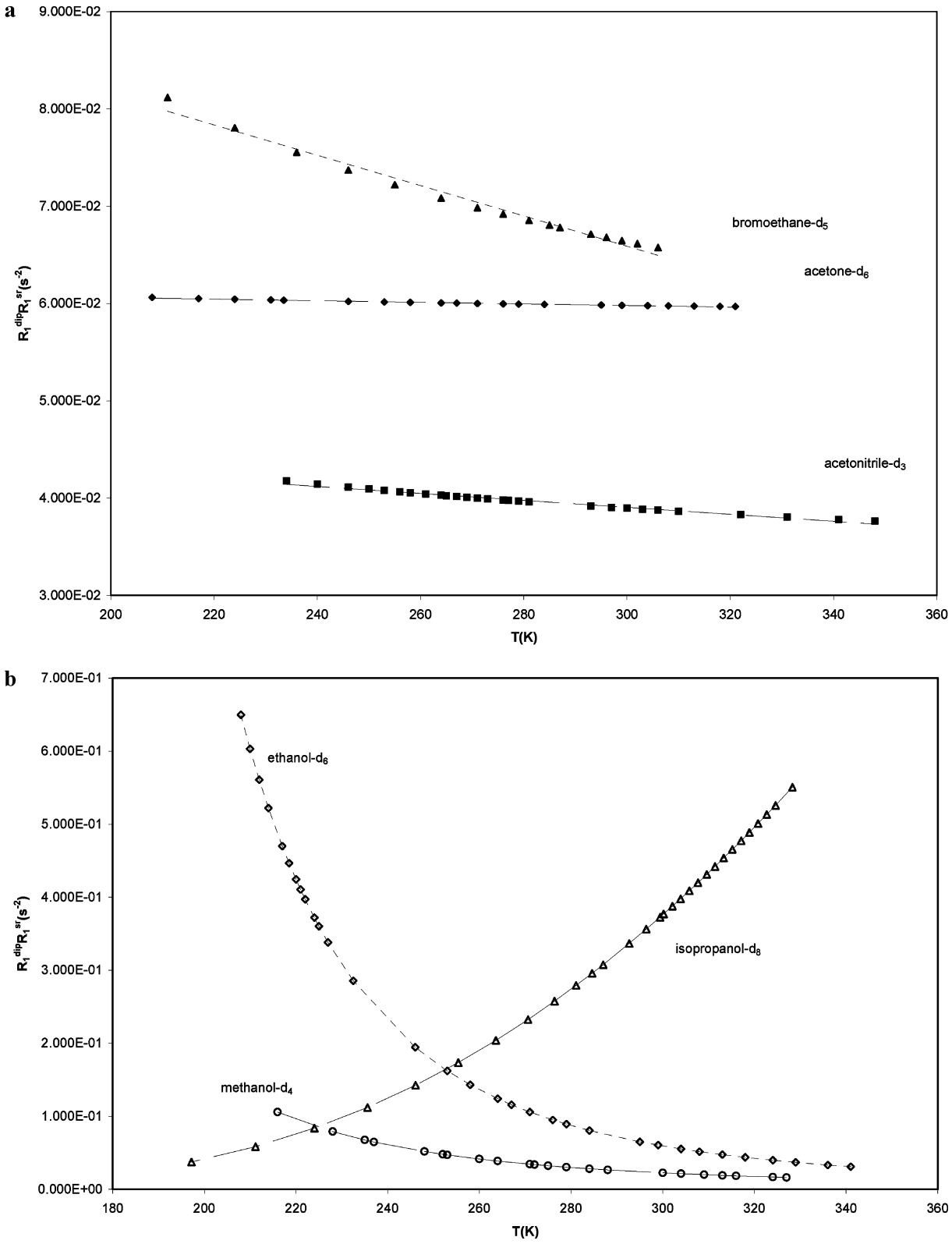

Figure 4. (a) Evolution, as a function of the absolute temperature, of the product $R_1^{dip.}R_1^{sr}$ where $R_1^{dip.}$ is the recalculated dipolar contribution and R_1^{sr} is the recalculated spin−rotation contribution (see text and eq 2) for hydrogen dissolved in acetone-d_6, acetonitrile-d_3, and bromoethane-d_5. Data concerning carbon disulfide are absent because $R_1^{dip.}$ is not available. Lines have been obtained by linear regression. (b) Evolution, as a function of the absolute temperature, of the product $R_1^{dip.}R_1^{sr}$ where $R_1^{dip.}$ is the recalculated dipolar contribution and R_1^{sr} is the recalculated spin−rotation contribution (see text and eq 2) for hydrogen dissolved in methanol-d_4, ethanol-d_6, and isopropanol-d_8. Lines are for visualization purposes.

eq 8. The T_{p-o} values obtained from these experimental data are gathered in Table 4.

The origin of the spin relaxation of a singlet state has been discussed in several places.[11,17,22−24] Here, we can simply state that it stems from *intermolecular* dipolar interactions giving rise to random fields. The relaxation rate involves three contributions: the spectral density associated with random fields at proton A, $J_{rf(A)}$, the spectral density associated with random

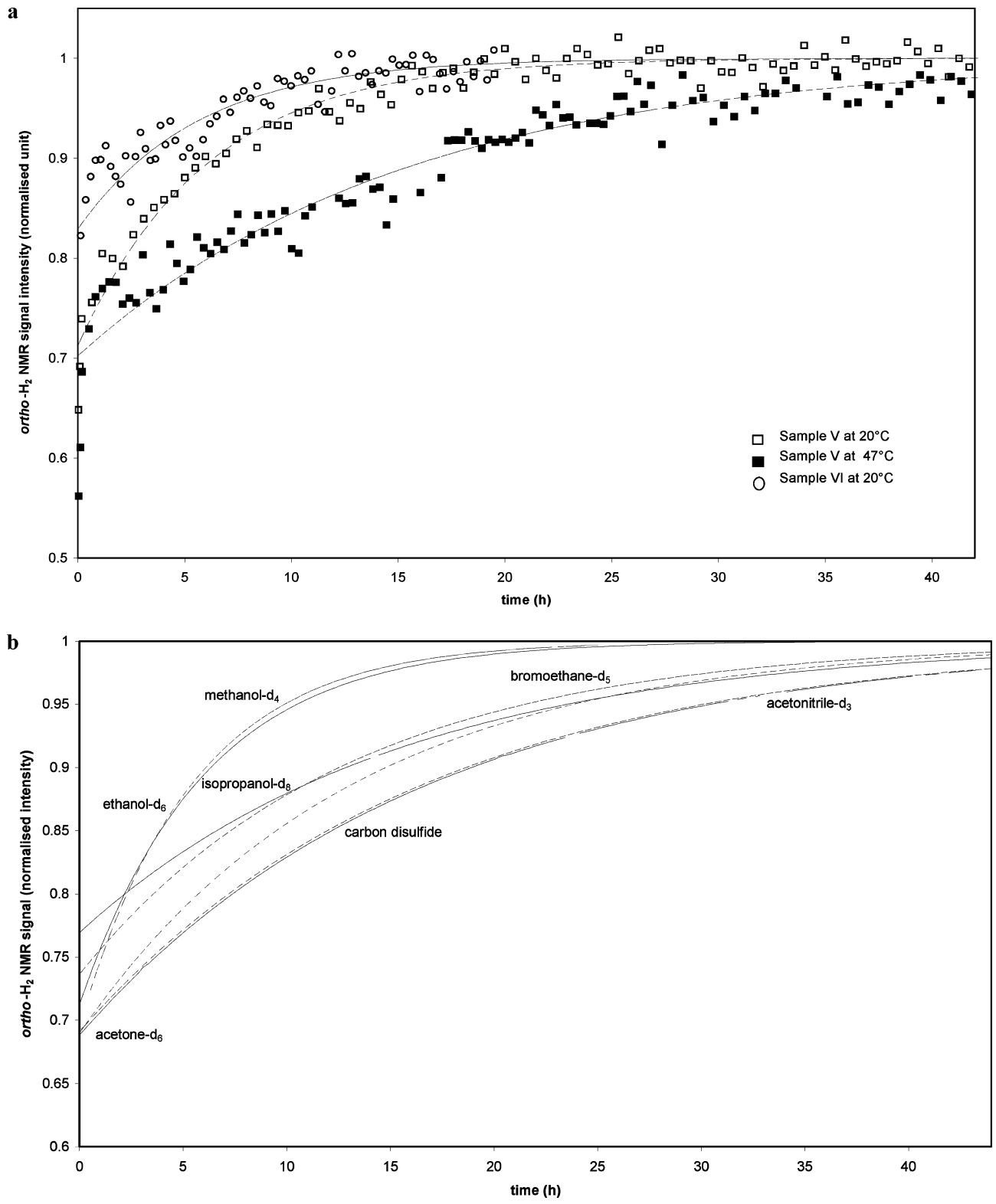

Figure 5. (a) Evolution, as a function of time, of the hydrogen molecule NMR signal, initially enriched in its *para*-isomer, dissolved in an organic solvent (here ethanol-d_6). Empty squares, empty circles, and full squares are respectively the experimental data points (see Table 4) recorded in "pure" ethanol-d_6 at ambient temperature, in "pure" ethanol-d_6 at a higher temperature (sample V), and with addition of copper (II) nitrate at ambient temperature (sample VI). The curves result from the fitting procedure described in the text. Data have been normalized to the equilibrium value. (b) Evolution at ambient temperature, as a function of time, of the hydrogen molecule NMR signals, initially enriched in its *para*-isomer, dissolved in the organic solvents considered in this work. The displayed curves are deduced by smoothing from experiments data points.

fields at proton A′, $J_{\mathrm{rf(A')}}$, and a spectral density describing the correlation of random fields at A and A′, $J^{\mathrm{cross}}_{\mathrm{rf(A),rf(A')}}$.

$$\frac{1}{T_{\mathrm{p-o}}} = 2J_{\mathrm{rf(A)}} + 2J_{\mathrm{rf(A')}} - 4J^{\mathrm{cross}}_{\mathrm{rf(A),rf(A')}} \qquad (9)$$

The latter is of sign opposite to that of the former and is twice their respective contributions. This means that, if by chance, the random fields at A and A′ are fully correlated (i.e., $J_{\mathrm{rf(A)}} = J_{\mathrm{rf(A')}} = J^{\mathrm{cross}}_{\mathrm{rf(A),rf(A')}}$), the relaxation rate describing the *para*−

TABLE 4: Time Constants for the *Para*−*Ortho* Back-Conversion, Identified with the Spin Relaxation Time of *Para*-Hydrogen

solvent	salt	sample	θ (°C)	T_{p-o} (h)[a]
acetone-d_6	no	I	20	11.1
acetonitrile-d_3	no	II	20	15.0
acetonitrile-d_3	no	II	47	17.2
methanol-d_4	no	III	20	5.3
methanol-d_4	no	III	47	7.9
methanol-d_4	$CuSO_4 \cdot 5H_2O$[c]	IV	20	1.6
ethanol-d_6	no	V	20	6.0
ethanol-d_6	no	V	47	15.3
ethanol-d_6	$Cu(NO_3)_2 \cdot 3H_2O$[c,d]	VI	20	2.2
ethanol-d_6	$Cu(NO_3)_2 \cdot 3H_2O$[c,d]	VII	20	5.6
isopropanol-d_8	no	VIII	20	15.4
bromoethane-d_5	no	IX	20	12.9
bromoethane-d_5	no	IX	30	12.8
carbon disulfide (+TMS[b])	no	X	20	15.0
carbon disulfide (+TMS[b])	no	X	40	16.6

[a] Experimental error on the values is estimated to be about 1 h. [b] The tetramethylsilane (TMS) ^{1}H NMR signal has been used as the internal reference. [c] Nonhydrated copper(II) salts are insoluble in the solvents studied here. [d] The concentration of Cu(II) ions in sample VII is one-third of the Cu(II) ion concentration in sample VI.

ortho conversion is null. Of course, this does not occur in practice, but this explains why T_{p-o} can be very long.

Indeed, the order of magnitude of T_{p-o} in liquids is about hours, generally greater than 10 h, and seems to be quite independent of the nature of the solvent, except in the case of methanol-d_4 and ethanol-d_6 for which it drops to about 6 h. Again, hydrogen bonds are likely to be responsible for this particular behavior, as they probably constitute a sort of lattice that favors different intermolecular dipolar interactions affecting A and A′ and which thus would lower the correlation of the corresponding random fields at A and A′ (see eq 9).

Moreover, as expected, the value of T_{p-o} decreases with the copper(II) ions concentration (see data of samples IV, VI, and VII), thus enlightening that paramagnetic species speed up the conversion phenomenon via increased dipolar interactions (due to the huge value of the electron magnetic moment) and the decrease of the correlation of corresponding random fields at A and A′. This is in accordance with the usual assumption concerning the *para*-enrichment phenomenon, which invokes paramagnetic species in charcoal and/or iron trioxide permitting the transitions to flow from the *ortho* to *para* states and *vice versa*, transitions which, for symmetry reasons, cannot be induced by electromagnetic radiations.[12,50,25,27,28] Finally, the increase of this relaxation time at higher temperature further supports the idea of intermolecular dipolar interactions that obviously decrease when the temperature increases. In fact, beyond the strength of the dipolar interactions, we must consider the last term in eq 9, which is able to cancel the first two terms (in the case of an almost perfect correlation). We can therefore understand that when the hydrogen molecule is in the vicinity of a medium sized molecule, the correlation is important (most solvents considered here). This correlation should decrease when the hydrogen molecule is embedded in a sort of lattice (methanol-d_4 and ethanol-d_6) because of the different moieties regularly spaced. Likewise, in the case of an ion (paramagnetic), the probability that this ion is at the center of the hydrogen molecule is weak and thus decreases the correlation term.

Conclusion

We have shown that spin relaxation of *ortho*-hydrogen dissolved in various solvents is as expected: it arises from spin−rotation (because hydrogen is a small molecule) and from intramolecular dipolar interaction (due to a short H−H bond length). We were able to separate both contributions and to determine relevant correlation times at each temperature. The dipolar correlation time varies linearly with η/T (η: viscosity of the solvent in which is dissolved hydrogen at the absolute temperature T) for all solvents investigated here except isopropanol-d_8 (and carbon disulfide for which the dipolar contribution cannot be determined). For nonalcoholic solvents, the Stokes−Einstein−Debye model (possibly with a microviscosity factor) seems to apply. There is a particular behavior for alcohols and more especially for isopropanol-d_8, attributed to the liquid-state complexity. Conversely, the classical Stokes−Einstein model accounts reasonably well for the translational diffusion. Concerning the spin−rotation correlation time, and according to Hubbard's theory, its product by the dipolar correlation time should be constant as a function of $1/T$. This occurs only for acetone-d_6 and, in that case, a spin−rotation constant in agreement with literature data is retrieved.

Concerning *para*-hydrogen, dissolved in the same solvents as *ortho*-hydrogen, we have to deal with spin relaxation of a singlet state. This singlet state has already been considered when the two protons are nonequivalent. It has been observed in several instances that relaxation, in that case, is very slow. We have demonstrated here that it is still much slower when the two nuclei involved in the singlet state are equivalent (due to the correlation term capable of canceling the direct terms; see eq 9). Indeed, experimental results have been actually interpreted along these lines by varying the nature of the solvent, the temperature, and/or the amount of paramagnetic species. The conclusion is that the back-conversion of *para*-isomer toward *ortho*-isomer may take several hours in liquids, whereas the time scale of this phenomenon is about days in the gas phase.[12,25−28]

Acknowledgment. This work has been supported by the European Community through the NEST Project "Adventure with Spin-Isomers: Separation, Physical Chemistry and Applications of *Ortho*- and *Para*-Water".

References and Notes

(1) Gilboa, H.; Chapman, B. E.; Kuchel, P. W. *J. Magn. Reson. A* **1996**, *119*, 1.

(2) Kuchel, P. W.; Chapman, B. E.; Lennon, A. J. *J. Magn. Reson. A* **1993**, *103*, 329.

(3) Sartori, E.; Ruzzi, M.; Turro, N. J.; Decatur, J. D.; Doetschman, D. C.; Lawler, R. G.; Buchachenko, A. L.; Murata, Y.; Komatsu, K. *J. Am. Chem. Soc*. **2006**, *128*, 14752.

(4) Hubbard, P. S. *Phys. Rev*. **1963**, *131*, 1155.

(5) McClung, R. E. D. *Encyclopedia of Nuclear Magnetic Resonance*; Wiley: New York, 1996; Vol. 8, p 4530.

(6) Bakhmutov, V. I. *Practical NMR Relaxation for Chemists*; Wiley: New York, 2004; Chapters 4 and 5.

(7) Canet, D. *Nuclear Magnetic Resonance: Concepts and Methods*; Wiley: New York, 1996.

(8) Dechter, J. J.; Polanco, O. R.; Kowalewski, J. *J. Magn. Reson.* **1985**, *65*, 395.

(9) Bodor, A.; Banyai, J.; Kowalewski, J.; Glaser, J. *Magn. Reson. Chem.* **2002**, *40*, 716.

(10) Kowalewski, J.; Mäler L. *Nuclear Spin Relaxation in Liquids: Theory, Experiments, and Applications*, CRC Press: Boca Raton, FL, 2006.

(11) Aroulanda, C.; Canet, D.; Mutzenhardt, P. Unpublished work presented during the second meeting of the EU supported NEST Project "Adventure with Nuclear Spin Isomers: Separation, Physical Chemistry and Applications of *Ortho* and *Para*-Water", March 17th, 2006, Turin, Italy.

(12) Bowers, C. R. *Encyclopedia of Nuclear Magnetic Resonance*; Wiley: New York, 2002; Vol. 9, p 750.

(13) Canet, D.; Aroulanda, C.; Mutzenhardt, P.; Aime, S.; Gobetto, R.; Reineri, F. *Concepts Magn. Reson. A* **2006**, *28*, 321.
(14) Aime, S.; Gobetto, R.; Reineri, F.; Canet, D. *J. Chem. Phys.* **2003**, *119*, 8890.
(15) Aime, S.; Gobetto, R.; Reineri, F.; Canet, D. *J. Magn. Reson.* **2006**, *178*, 184.
(16) Aime, S.; Gobetto, R.; Canet, D. *J. Am. Chem. Soc.* **1998**, *120*, 6770.
(17) Canet, D.; Bouguet-Bonnet, S.; Aroulanda, C.; Reineri, F. *J. Am. Chem. Soc.* **2007**, *129*, 1445.
(18) Koptyug, I. V.; Kovtunov, K. V.; Burt, S. R.; Anwar, M. S.; Hilty, C.; Han, S-I.; Pines, A.; Sagdeev, R. Z. *J. Am. Chem. Soc.* **2007**, *129*, 5580.
(19) Golman, K.; Axelsson, O.; Jo'hannesson, H.; Månsson, S.; Olofsson, C.; Petersson, J. S. *Magn. Reson. Med.* **2001**, *46*, 1.
(20) Bouchard, L-S.; Kovtunov, K. V.; Burt, S. R.; Anwar, M. S.; Koptyug, I. V.; Sagdeev, R. Z.; Pines, A. *Ang. Chem. Int. Ed.* **2007**, *46*, 4064.
(21) Bhattacharya, P.; Chekmenev, E. Y.; Perman, W. H.; Harris, K. C.; Lin, A. P.; Norton, V. A.; Tan, C. T.; Ross, B. D.; Weitekamp, D. P. *J. Magn. Reson.* **2007**, *186*, 150.
(22) Carravetta, M.; Levitt, M. H. *J. Am. Chem. Soc.* **2004**, *126*, 6229.
(23) Carravetta, M.; Levitt, M. H. *J. Chem. Phys*. **2005**, *122*, 214505.
(24) Pileio, G.; Concistrè, M.; Carravetta, M.; Levitt, M. H. *J. Magn. Reson.* **2006**, *182*, 353.
(25) Trasca, R. A.; Kostov, M. K.; Cole, M. W. *Phys. Rev. B* **2003**, *67*, 035410.
(26) Grinev, T. A.; Buchachenko, A. A.; Krems, R. V. *ChemPhysChem* **2007**, *8*, 815.
(27) Sandler, Y. L. *J. Phys. Chem.* **1954**, *58*, 58.
(28) Sandler, Y. L. *J. Phys. Chem.* **1954**, *58*, 54.
(29) Komasa, J.; Rychlewski, J.; Raynes, W. T. *Chem. Phys. Lett.* **1995**, *236*, 19.
(30) Komasa, J.; Cencek, W.; Rychlewski, J. *Phys. Rev. A* **1992**, *46*, 2351.
(31) Sundholm, D.; Gauss, J.; Ahlrichs, R. *Chem. Phys. Lett.* **1995**, *243*, 264.
(32) Sundholm, D.; Gauss, J.; Schäfer, A. *J. Chem. Phys.* **1996**, *105*, 11051.
(33) Reid, R. V.; Chu, A. H.-M. *Phys. Rev. A* **1974**, *9*, 609.
(34) Flygare, W. H. *Chem. Rev.* **1974**, *74*, 653.
(35) Gierke, T. D.; Flygare, W. H. *J. Am. Chem. Soc.* **1972**, *94*, 7277.
(36) Bryce, D. L.; Wasylishen, R. E. *Acc. Chem. Res*. **2003**, *36*, 327.
(37) *Handbook of Chemistry and Physics*, 83rd ed.; CRC Press: Boca Raton, FL, 2002−2003; p 6-184.
(38) Telang, M. S. *J. Phys. Chem.* **1946**, 373.
(39) Woessner, D. E. *Encycl. NMR Spectrosc.* **1996**, 1068.
(40) Wakai, C.; Nakahara, M. *J. Chem. Phys.* **1997**, *106*, 7512.
(41) Price, W. S.; Ide, H.; Arata, Y. *J. Chem. Phys.* **2000**, *113*, 3686.
(42) Bondi, A. *J. Phys. Chem*. **1964**, *68*, 441.
(43) Boeré, R. T.; Kidd, R. G. *Annu. Rep. NMR Spectrosc.* **1982**, *13*, 319.
(44) Gierer, A.; Wirtz, K. *Z. Naturforsch. A* **1953**, *8*, 532.
(45) Hu, C.-M.; Zwanzig, R. *J. Chem. Phys.* **1974**, *60*, 4354.
(46) Youngren, G. K.; Acrivos, A. *J. Chem. Phys.* **1975**, *63*, 3846.
(47) Larive, C. K.; Lin, M.; Kinnear, B. S.; Piersma, B. J.; Keller, C. E.; Carper, W. R. *J. Phys. Chem. B* **1998**, *102*, 1717.
(48) Irwin, A. D.; Assink, R. A.; Henderson, C. C.; Cahill, P. A. *J. Phys. Chem.* **1994**, *98*, 11832.
(49) Sharp, R. R. *J. Chem. Phys.* **1972**, *57*, 5321.
(50) Matsumoto, M.; Espenson, J. H. *J. Am. Chem. Soc.* **2005**, *127*, 11447.